Journal of Power Sources 184 (2008) 361–369

Contents lists available at ScienceDirect

Journal of Power Sources

journal homepage: www.elsevier.com/locate/jpowsour

Polyoxometallate-stabilized Pt–Ru catalysts on multiwalled carbon nanotubes: Influence of preparation conditions on the performance of direct methanol fuel cells

D.M. Han[a,b], Z.P. Guo[a,*], Z.W. Zhao[a], R. Zeng[a], Y.Z. Meng[b,*], D. Shu[c], H.K. Liu[a]

[a] Institute for Superconducting and Electronic Materials, University of Wollongong, NSW 2522, Australia
[b] Institute of Energy & Environment Materials, School of Physics & Engineering, Sun Yat-Sen University, Guangzhou, PR China
[c] Department of Chemistry, South China Normal University, Guangzhou, PR China

ARTICLE INFO

Article history:
Received 30 December 2007
Received in revised form 26 February 2008
Accepted 17 March 2008
Available online 29 March 2008

Keywords:
DMFC
Pt–Ru catalyst
PMo_{12}
Microwave heating
Preparation conditions
Electrocatalytic activity

ABSTRACT

A novel catalyst, polyoxometallate-stabilized platinum–ruthenium alloy nanoparticles supported on multiwalled carbon nanotubes (Pt–Ru–PMo_{12}-MWNTs), was synthesized by a microwave-assisted polyol process. The effects of microwave reaction time, microwave reaction power, and pH value of the reaction solution on the electrocatalytic properties of Pt–Ru–PMo_{12}-MWNTs catalysts were also investigated. The polyoxometallate (PMo_{12}) formed a self-assembled monolayer on the surface of the Pt/Ru nanoparticles and MWNTs, which effectively prevented the agglomeration of Pt, Ru nanoparticles and MWNTs, due to the electrostatic repulsive interactions between the negatively charged PMo_{12} monolayers. Energy dispersive spectroscopy examination and electrochemical measurements showed that the loading content of Pt/Ru and their electrochemical activity vary with the synthesis conditions, such as pH, reaction time, and microwave power. It was found that the a Pt–Ru–PMo_{12}-MWNTs electrocatalyst with high Pt loading content, small crystallite size, and good electrocatalytic activity could be synthesized using a long reaction time, intermediate microwave power, and a pH value of 7. The electrocatalysts obtained were characterized using X-ray diffraction, and scanning and transmission electron microscopy. Their electrocatalytic properties were also investigated by using the cyclic voltammetry technique.

1. Introduction

Over the past decade, the direct methanol fuel cell (DMFC) has been receiving increasing attention as a future power source for small portable electronic devices, such as laptops and mobile telephones, due to its advantages, such as easy fuel storage, simple structure, reduced system weight, high energy efficiency, and low emissions [1–7]. It has been recognized that the success of fuel cell technology depends largely on two key materials: the electrocatalyst and the membrane [8]. This means that slow anode kinetics need to be overcome by developing new anode catalysts and that methanol crossover needs to be overcome by developing new membranes. So, one of the most important tasks in the DMFC field is to develop anode catalysts with high activity, reasonable reliability, and durability, in combination with cost reduction. To improve DMFC anode catalyst performance, the exploration of new catalyst materials, including noble and non-noble metals, has been a focus for many researchers.

At this stage, the most promising anode materials for DMFCs are Pt–Ru bimetallic catalysts dispersed on carbon. As reviewed by Arico et al. [9] and Lamy et al. [10], many works have been devoted to the optimization of Pt–Ru catalyst performance towards methanol oxidation. So far as the mechanism of methanol oxidation is concerned, it is generally accepted that it is the Pt sites in the Pt–Ru alloys that are primarily involved in both the methanol dehydrogenation step and in the strong chemisorption of methanol residues. At a suitable electrodepotential (0.2 V vs. reference hydrogen electrode (RHE)), water discharging occurs on Ru sites with the formation of Ru-OH groups at the catalyst surface [11]:

$$Ru + H_2O \rightarrow Ru\text{-}OH + H^+ + 1e^- \quad (1)$$

The final step is the reaction of Ru-OH groups with neighboring methanolic residues adsorbed on Pt to give carbon dioxide:

$$Ru\text{-}OH + Pt\text{–}CO \rightarrow Ru + Pt + CO_2 + H^+ + 1e^- \quad (2)$$

So, this type of catalyst is favored because of (i) its high activity towards methanol oxidation and (ii) its water activation, which

* Corresponding authors. Fax: +61 2 4221 5731.
E-mail addresses: zguo@uow.edu.au (Z.P. Guo), mengyzh@mail.sysu.edu.cn (Y.Z. Meng).

0378-7753/$ – see front matter © 2008 Elsevier B.V. All rights reserved.
doi:10.1016/j.jpowsour.2008.03.051

is critical for removal of the strongly adsorbed CO that is formed during the decomposition of methanol. Ruthenium has a more negative potential than Pt, thus weakening the bonds between CO and Pt, which will increase the possibility of oxidizing the CO molecules and providing more surface sites for methanol oxidation [12].

However, platinum and ruthenium are noble metals and have a low natural abundance, which is a significant barrier to the widespread commercialization of DMFC. It is important to reduce the amount of precious metals and improve the activity of Pt/Ru alloy catalysts. In order to achieve high electrocatalyst activity and to reduce the cost of the electrode, highly distributed catalyst nanoparticles with small size and narrow size distribution must be prepared. In addition, an efficient support, which is capable of forming triple phase boundaries (electrode/electrolyte/gas), is also necessary. Carbon nanotubes (CNTs) have been considered to be attractive support materials for noble metal nanoparticles, due to their unique electrical and structural properties, such as high tensile strength coupled with high surface area, high electric conductivity, and high thermal conductivity [13–15]. CNTs with a three-dimensional structure are efficient for diffusion of fuel and increase the contact area between catalyst and fuel. However, it is difficult to decorate metal nanoparticles on the surface of CNTs with uniform size and good dispersion. One of the reasons for this is that the metal nanoparticles are spontaneously formed at the defect sites on the surface of CNTs. Moreover, CNTs tend to agglomerate without any pretreatments.

Polyoxometallates ($H_3PMo_{12}O_{40}$, PMo_{12}) are known to form self-assembled monolayers on common solid electrodes [16,17]. Keggin-type heteropolyanions of molybdenum are particularly attractive because of their ability to adsorb irreversibly on carbon and metal surfaces to form structured films. PMo_{12} has been used as a soluble molecular species in catalysis and biomedicine, in the form of coatings on metals such as aluminum or silver. It can be imagined that if we coat the CNTs and metals with a polyoxometallate monolayer, the agglomeration of metal nanoparticles and the distribution of CNTs could be effectively prevented. On the other hand, electrocatalyst formulations, which include molybdenum, have been reported [18,19]. It was thought that molybdenum would be able to take advantage of proper surface promoters that can facilitate labile adsorption of methanol residues and their oxidation through redox functionalities [9]. In an acid electrolyte environment, molybdenum is generally stable in one or more oxidized forms and can easily change oxidation states by adsorbing hydroxyl ions from water and donating these species to methanol residues adsorbed on platinum. Lamy and LØger [19] have shown that the Pt–Ru–Mo system shows good electrocatalytic activity. However, the electrochemical stability of molybdenum under prolonged operation has still not been demonstrated. Up to now, there have only been a few reports about the performance of electrocatalysts containing molybdenum.

In our previous work, Pt–PMo_{12}-MWNTs electrocatalysts with well-dispersed Pt nanoparticles and a monolayer of PMo_{12} on multiwalled carbon nanotubes (MWNTs) were successfully prepared [20]. The as-prepared Pt–PMo_{12}-MWNTs materials showed much higher electrocatalytic activity, higher cycle stability, and better tolerance to poisoning species in methanol oxidation than Pt-MWNTs catalysts prepared by the same method. In this paper, to further improve the electrocatalytic performance of PMo_{12}-stablized Pt-MWNTs catalysts for methanol oxidation, Pt–Ru–PMo_{12}-MWNTs catalysts were synthesized by the same method, i.e. the microwave-assisted polyol process. To the best of our knowledge, this is the first study on Pt–Ru–PMo_{12}-MWNTs nanoelectrocatalysts for DMFC applications. The effects of microwave reaction time, microwave reaction power, and the pH value of the reaction solution on the electrocatalytic performance of Pt–Ru–PMo_{12}-MWNTs catalysts were also systematically investigated.

2. Experimental

2.1. Microwave heated synthesis of Pt–Ru–PMo_{12}-MWNTs

The MWNTs were prepared by catalytic chemical vapor deposition (CVD), using nanosized cobalt as the catalyst [21]. The MWNTs were treated in concentrated HNO_3 at 393 K for 2 h. Then, the mixture was diluted with water, filtered, washed with excess deionized water, and dried at 60 °C in a vacuum oven. Pt–Ru–PMo_{12}-MWNTs catalysts were prepared by microwave heating of an ethylene glycol (EG) solution of $H_3PMo_{12}O_{40}$(PMo_{12}), $H_2PtCl_6{\cdot}6H_2O$, and $RuCl_3{\cdot}xH_2O$ with MWNTs suspended in the solution. A typical preparation would consist of the following steps: 400 mg pretreated MWNTs, 200 mg PMo_{12}, 15 ml of 0.05 M $H_2PtCl_6{\cdot}6H_2O$ (Aldrich, A.C.S. Reagent) EG solution, 15 ml of 0.05 M $RuCl_3{\cdot}xH_2O$ (Aldrich, A.C.S. Reagent) EG solution, and 30 ml of 0.04 M KOH were mixed with 100 ml of EG (Aldrich) in a beaker and ultrasonicated with an ultrasonic probe for 4 h. 0.004 M KOH was used to adjust the pH value of the solution. The suspension was separated into four equal parts and immediately transferred to a household microwave. The suspensions were placed in the center of the microwave oven and heated according to the times and the powers listed in Table 1. The Pt and Ru nanoparticles were precipitated from the solution and deposited on the surface of the MWNTs. The as-prepared suspension was filtered, and the obtained Pt–Ru–PMo_{12}-MWNTs samples were washed three times each with acetone and deionized water. The products were dried under vacuum at 60 °C.

2.2. Characterization of microwave synthesized Pt–Ru–PMo_{12}-MWNTs catalysts

The morphologies and distributions of Pt, Ru nanoparticles decorated on the surfaces of the MWNTs were investigated by scanning electron microscopy (SEM) using a JEOL JSM-6460A instrument, with additional semi-quantitative information obtained using large area standardless energy dispersive spectroscopy (EDS) analysis. Transmission electron microscopy (TEM) was performed using a

Table 1
Experimental conditions for the preparation of the Pt–Ru–PMo_{12}-MWNTs catalysts

	Reaction time (s)	Microwave power (W)	pH value
Sample 1	52	800	4
Sample 2	70	800	4
Sample 3	84	800	4
Sample 4	102	800	4
Sample 5	84	640	4
Sample 6	84	480	4
Sample 7	84	320	4
Sample 8	84	160	4
Sample 9	84	800	5
Sample 10	84	800	7
Sample 11	84	800	9
Sample 12	84	800	10
Sample 13	52	800	7
Sample 14	70	800	7
Sample 15	102	800	7
Sample 16	102	640	7
Sample 17	102	480	7
Sample 18	102	320	7

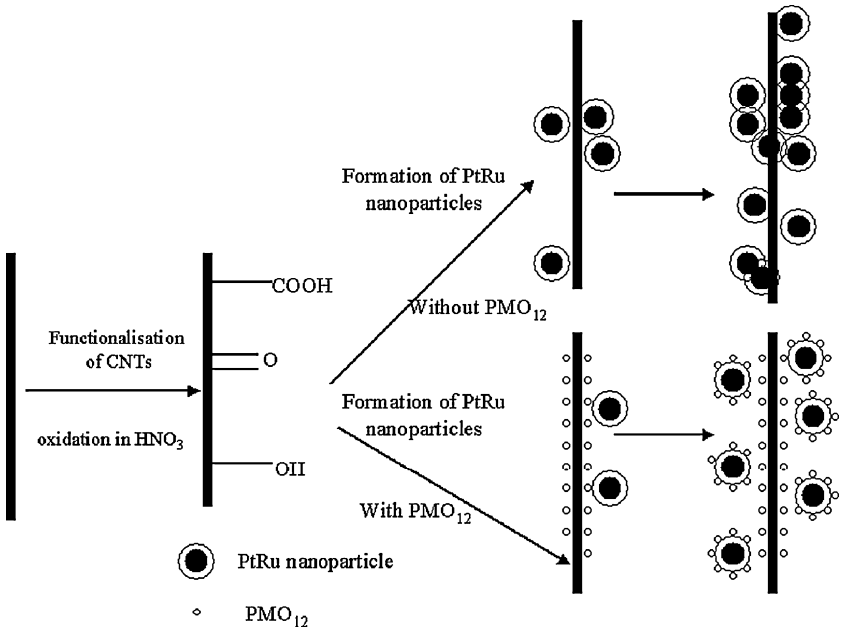

Fig. 1. Schematic diagram illustrating the synthesis of Pt–Ru–PMo_{12}-MWNTs catalysts.

JEOL JEM 2011. TEM samples were dispersed on lacey carbon support films. X-ray diffraction (XRD) patterns were obtained with a Phillips PW1730 generator and diffractometer using Cu Kα radiation and a graphite monochromator. XRD peaks associated with Pt nanoparticles were quite broad, and a weighted average of the incident Cu Kα1 and Cu Kα2 wavelengths of $\lambda_{av} = 0.154184$ nm was assumed.

2.3. Electrochemical measurements

All the electrochemical experiments were performed on a CHI 660 Electrochemical Workstation. A three-electrode system was employed with an Ag/AgCl electrode as the reference electrode, a platinum wire as the counter electrode, and a glassy carbon (GC) electrode (with area of 0.0314 cm^2) as the working electrode. The

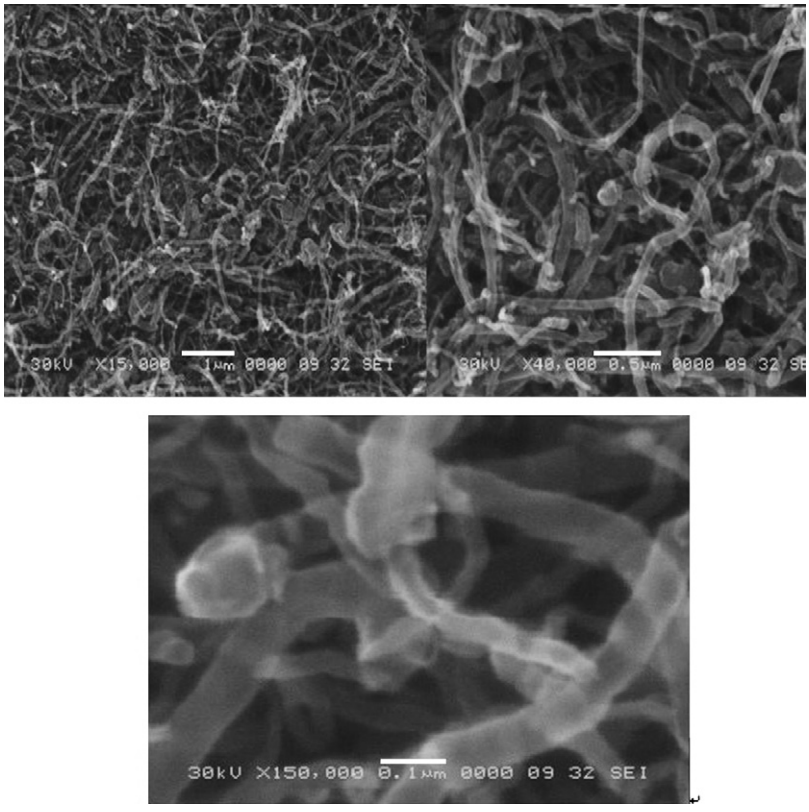

Fig. 2. Typical SEM images of Pt–Ru–PMo_{12}-MWNTs catalysts.

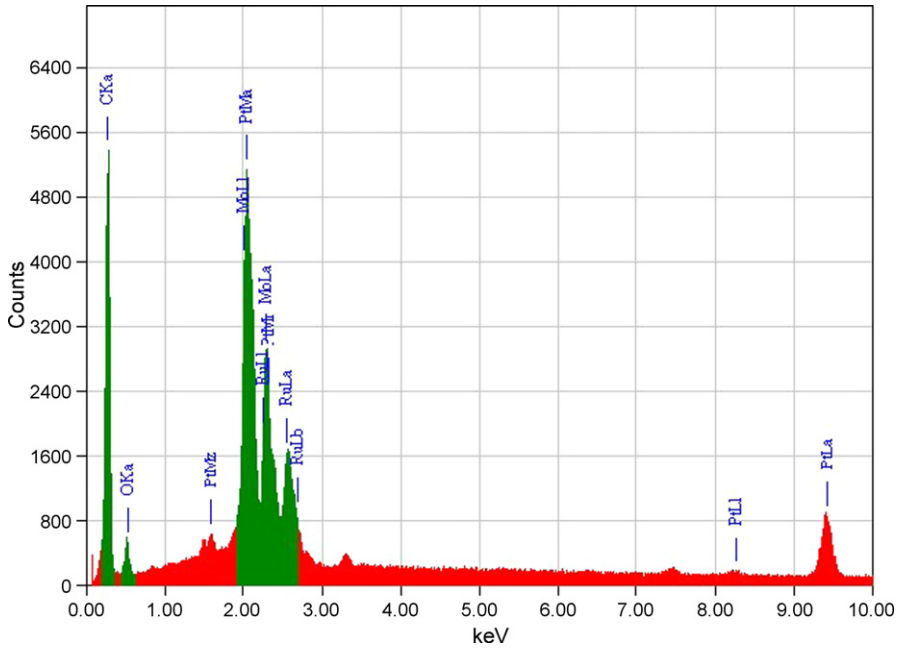

Fig. 3. Typical EDS pattern of Pt–Ru–PMo_{12}-MWNTs catalysts.

electrolyte solutions (0.5 M H_2SO_4 or 0.5 M H_2SO_4 + 0.5 M CH_3OH) were de-aerated in high purity Ar before measurements. All measurements were carried out at room temperature. The GC-catalyst electrode was prepared by the following procedure: (a) the GC electrode (surface area) was washed with water and acetone; (b) a solution was made by sonicating 2 mg catalyst and 1 mL de-ionized water; (c) 10 μL of 2 mg mL^{-1} catalyst solution was added to the surface of the GC electrode and dried in air.

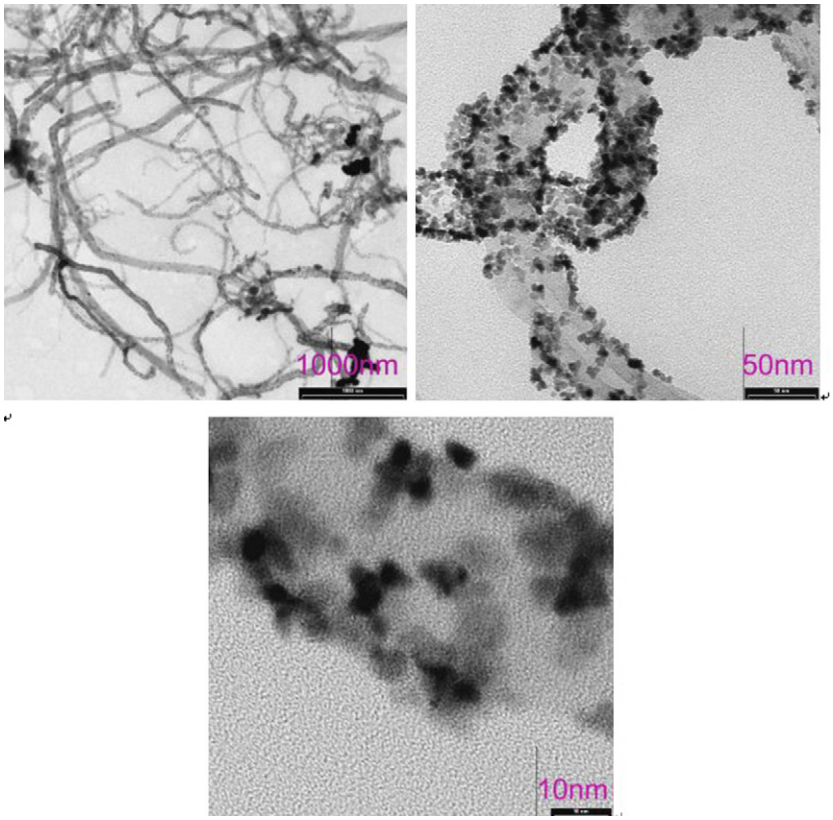

Fig. 4. Typical TEM images of Pt–Ru–PMo_{12}-MWNTs catalysts.

Table 2
Loading content of metal elements for synthesized Pt–Ru–PMo_{12}-MWNTs catalysts

	Sample 1	Sample 2	Sample 3	Sample 4
Pt wt%	22.36	19.02	44.99	47.27
Ru wt%	3.21	2.79	11.01	12.39
Mo wt%	5.98	5.27	17.56	17.55
Pt:Ru atom ratio	1.95:0.54	1.58:0.45	8.54:4.04	10.33:5.65
	Sample 5	Sample 6	Sample 7	Sample 8
Pt wt%	25.44	24.49	13.54	0.27
Ru wt%	4.08	2.8	0.02	0
Mo wt%	7.74	9.48	1.8	0.54
Pt:Ru atom ratio	2.42:0.75	2.32:0.51	0.98:0	0.02:0
	Sample 9	Sample 10	Sample 11	Sample 12
Pt wt%	29.73	21.02	12.34	5.56
Ru wt%	4.46	3.28	1.34	0.04
Mo wt%	7.86	5.87	1.92	1.31
Pt:Ru atom ratio	2.32:0.87	1.82:0.65	0.97:0.34	0.44:0

3. Results and discussion

3.1. Microstructural characterization

Since MWNTs have a hydrophobic surface, they tend to aggregate in polar solvent. In order to deposit a large amount of Pt, Ru nanoparticles with uniform distribution, the surface of the MWNTs must be modified. One common method used to modify the MWNTs' surface is oxidation treatment. It was found that oxidation treatment of MWNTs by a strong acid, such as H_2SO_4/HNO_3, could produce oxygen-containing groups (–COOH, –C=O, etc.), which can modify the hydrophobicity and inertness of the MWNT surface. Thus the Pt and Ru nanoparticles deposited on the MWNT surface, which has been treated with H_2SO_4/HNO_3, are small and relatively uniform. Another useful strategy to achieve a more uniform Pt nanoparticle distribution on MWNTs is by using polyoxometallate (PMo_{12}) to assist. Due to the nature of its ability to form self-assembled monolayers on the surface of MWNTs or hard metals and its negatively charged property, the PMo_{12} can effectively prevent the aggregation of metal nanoparticles on the MWNTs, while the monolayer-coating of PMo_{12} on MWNTs can also decrease the degree of tangling for the MWNTs, thus providing more usable space for Pt deposition. The PtRu alloy nanoparticle deposition process is schematically illustrated in Fig. 1. Typical SEM images of Pt–Ru–PMo_{12}-MWNT catalysts are shown in Fig. 2.

It can be seen that MWNTs in the Pt–Ru–PMo_{12}-MWNTs are well separated from each other and exhibit 'untangled' morphology. The existence of electrostatic repulsive interactions between the negatively charged PMo_{12} monolayers on the metal surfaces and the outer walls of the MWNTs could effectively prevent the agglomeration of metal particles and MWNTs. The amount of metal elements loaded on the MWNT supports was also estimated by semi-quantitative EDS. A typical EDS pattern of Pt–Ru–PMo_{12}-MWNTs catalyst is shown in Fig. 3. It indicates the presence of Ru and Mo.

It was found that the loading content of metals was affected by the pH value, microwave power, and reaction time. The amount of the Pt/Ru nanoparticle catalyst loaded on the MWNTs supports is listed in Table 2. From Table 2, it is obvious that the Pt loading content is significantly influenced by the reaction time, the microwave power, and the pH value. With an increase in the reaction time from 52 to 102 s, the loading amount of Pt increases from 22.36 to 47.27 wt%. With an increase in the microwave power from 160 to 800 W, the loading content of Pt increases from 0.27 to 44.99 wt%. However, the Pt content in the electrocatalysts decreases with increasing pH value. The atomic ratio of Pt to Ru is also influenced by the reaction time and the microwave power. When the reaction time increases from 52 to 102 s, the atomic ratio of Pt to Ru decreases from 1.95:0.54 (3.61:1) to 10.33:5.65 (1.83:1), and the relevant catalytic activity increases accordingly (Fig. 6(a)). The atomic ratio of Pt to Ru decreases with increasing microwave power, while the atomic ratio changes only slightly with changes in the pH value.

The general distribution of PtRu nanoparticles on the surfaces of the MWNTs is illustrated in the TEM images shown in Fig. 4. The surfaces of the MWNTs were uniformly decorated by PtRu nanoparticles, shown in the low resolution and high resolution images, with average particle sizes around 1–4 nm. It is generally agreed that the size of metal nanoparticles is determined by the rate of reduction of the metal precursor. The dielectric constant (41.4 at 298 K) and the dielectric loss of ethylene glycol are high, and hence rapid heating occurs easily under microwave irradiation. Fast heating rates can accelerate the formation of the metal nanoparticles, and the uniform microwave irradiation provides more homogeneous circumstances for their nucleation and growth.

The XRD patterns of the Pt–Ru–PMo_{12}-MWNTs catalysts are shown in Fig. 5. The effect of reaction time, microwave power, and pH values of the precursor solutions on the samples were investigated and are shown in Fig. 5(a), (b), and (c), respectively. The peak at 26.38° corresponds to the (0 0 2) planes of graphitized MWNT. It can be seen that the crystal structure of Pt in the catalysts is face-centered cubic, which is confirmed by the peaks at 39.86°, 46.6°, 67.48°, 81.88°, and 85.62°. These peaks are assigned to Pt(1 1 1), Pt(2 0 0), Pt(2 2 0), Pt(3 1 1), and Pt(2 2 2), respectively. XRD spectra for all the samples only showed the characteristic Pt fcc pattern and did not show any peaks related to tetragonal RuO_2 or hexagonal close-packed (hcp) Ru phases. It is believed [24] that this phenomenon indicates the absence of metallic Ru and the presence of un-alloyed Ru, most probably in amorphous oxide states. The results agreed well with other reports in the literature [25,26]. Since the Pt(2 2 0) peak is isolated from the MWNT-support diffraction peaks, the mean particle size of the Pt can be calculated from the (2 2 0) peak according to Scherrer's formula:

$$L = \frac{0.89\lambda_{K\alpha 1}}{\beta_{2\theta}\cos\theta_{max}}$$

where L is the mean size of the Pt particles, $\lambda_{K\alpha 1}$ is the X-ray wavelength (Cu Kα $\lambda_{K\alpha 1}$ = 0.154184 nm), θ_{max} is the maximum angle of the (2 2 0) peak, and $\beta_{2\theta}$ is the half-peak width for Pt(2 2 0) in radians. The calculated mean crystallite sizes of the samples are also shown in Fig. 5. It was found that the crystallite size of PtRu cata-

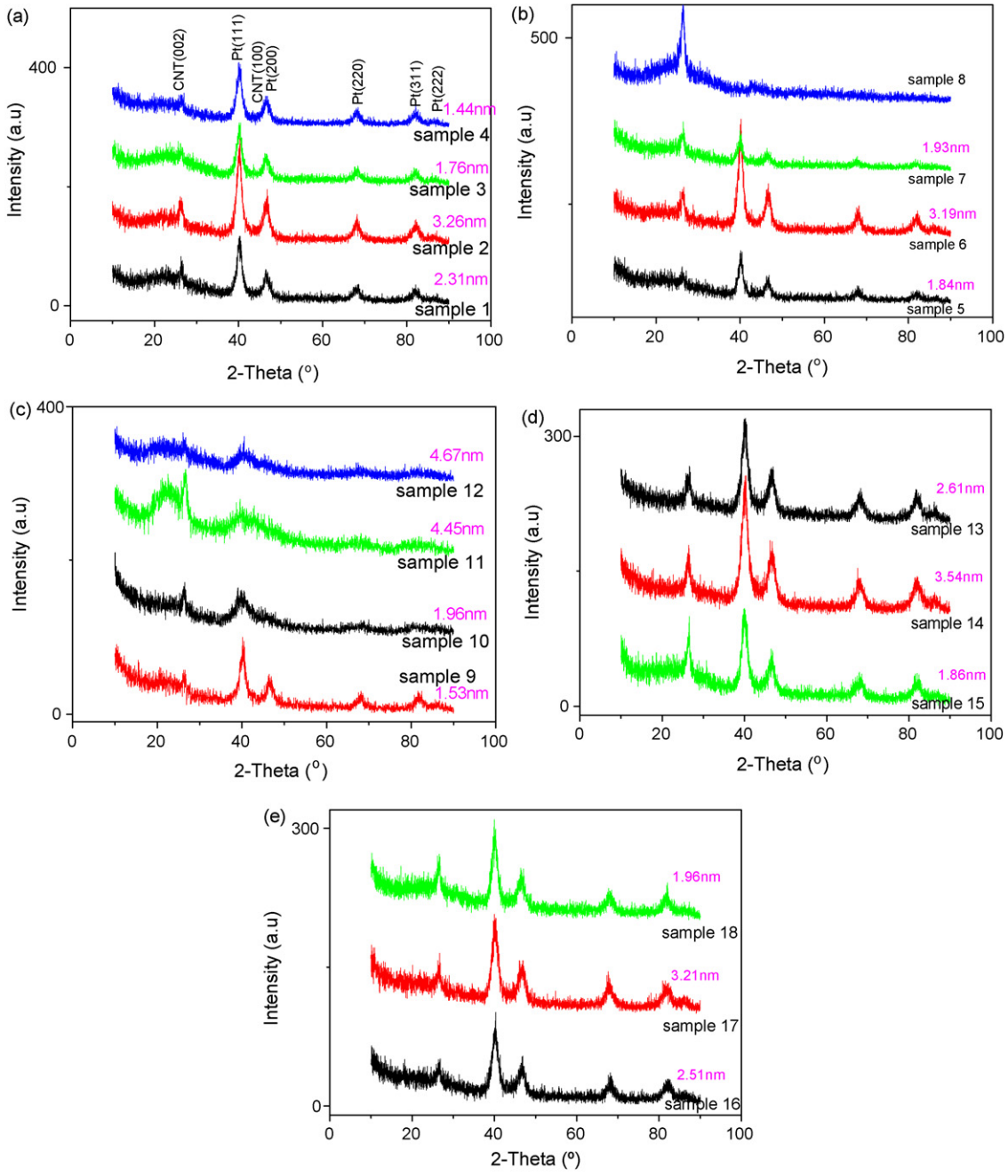

Fig. 5. X-ray diffraction patterns of Pt–Ru–PMo_{12}-MWNTs catalysts: (a) effect of reaction time, (b) effect of microwave power, and (c) effect of pH value. Pt–Ru–PMo_{12}-MWNTs catalysts synthesized at a pH value of 7: (d) effect of reaction time and (e) effect of microwave power.

lyst was significantly influenced by the pH value and the microwave power. The crystallite size increases with increasing pH values, while the crystallite size of PtRu alloy increases first, then decreases with increasing microwave power. A possible reason for this phenomenon is that there are both crystal core formation and a crystal growth process involved in PtRu deposition. When the microwave power is low, the crystal growth is slow. However, when the power is too high, there are a large amount of crystal cores generated, which also hinders the growth and the formation of large crystals. Sample 8 shows no characteristic Pt XRD peaks, suggesting that the microwave power (160 W) used in the synthesis is too weak to generate enough heat for H_2PtCl_6 reduction. The XRD patterns of Pt–Ru–PMo_{12}-MWNTs catalysts synthesized at a pH value of 7 are also shown in Fig. 5. The effects of the reaction time and microwave power on the samples were investigated and are shown in Fig. 5(d) and (e). It is found that the particle size of the PtRu alloy in these samples increases with increasing reaction time, while it increases first, then decreases when the microwave power is increased.

3.2. *Electrochemical performance of Pt–Ru–PMo_{12}-MWNTs electrocatalysts*

The electrocatalytic properties of the as-prepared Pt–Ru–PMo_{12}-MWNTs catalysts for the methanol oxidation reaction have also been characterized by cyclic voltammetry (CV) in Ar saturated 0.5 M H_2SO_4 and 0.5 M H_2SO_4 + 0.5 M MeOH solutions, respectively. Fig. 6 shows CV curves of the Pt–Ru–PMo_{12}-MWNTs

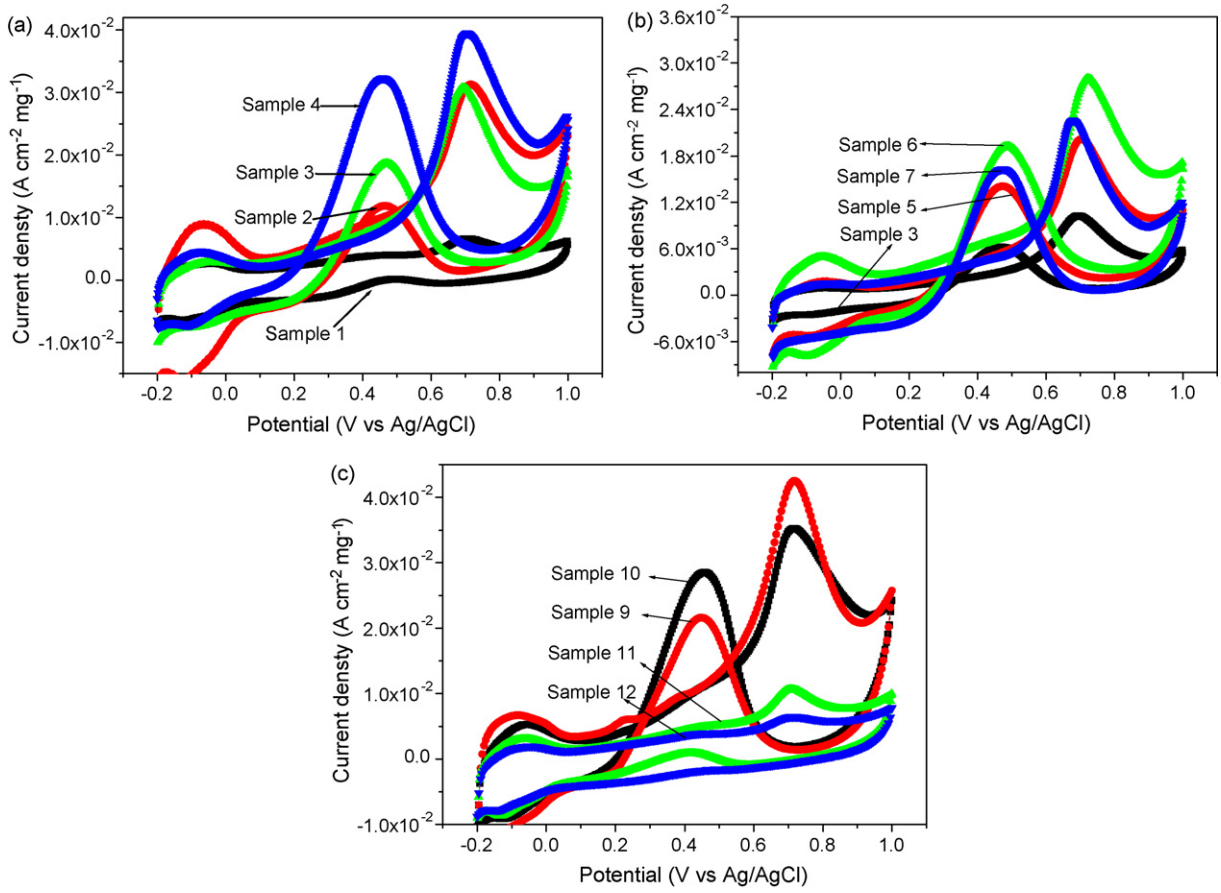

Fig. 6. Cyclic voltammograms of the Pt–Ru–PMo_{12}-MWNT catalysts in 0.5 M H_2SO_4 + 0.5 M CH_3OH electrolyte at the 125th cycle, collected at a scan rate of 200 mV s^{-1}: (a) effect of reaction time; (b) effect of microwave power; (c) effect of pH value.

catalysts at the 125th cycle. CV curves for samples prepared using different reaction times, microwave powers, and pH values are shown in Fig. 6(a), (b), and (c), respectively. There is a oxidation peak at about 0.7 V in the forward scan, which corresponds to the oxidation of methanol, while in the reverse scan, the adsorbed intermediates produce a second oxidation peak at around 0.45 V [22]. The anodic peak in the reverse scan was attributed to the removal of the incompletely oxidized carbonaceous species formed in the forward scan. These carbonaceous species are mostly in the form of linearly bonded Pt=C=O. The residual carbon species are oxidized according to the following reaction:

$$PtOH_{ad} + Pt{=}C{=}O \rightarrow CO_2 + 2Pt + H^+ + e^- \quad (3)$$

The voltammetric features are in good agreement with the literature [23,27].

It is obvious that the intensity of the oxidation peaks increases with increasing reaction time (Fig. 6(a)), indicating a higher loading content of PtRu on the MWNTs for the samples prepared with longer reaction time, which is consistent with the EDS analysis results. The microwave power shows no clear effect on

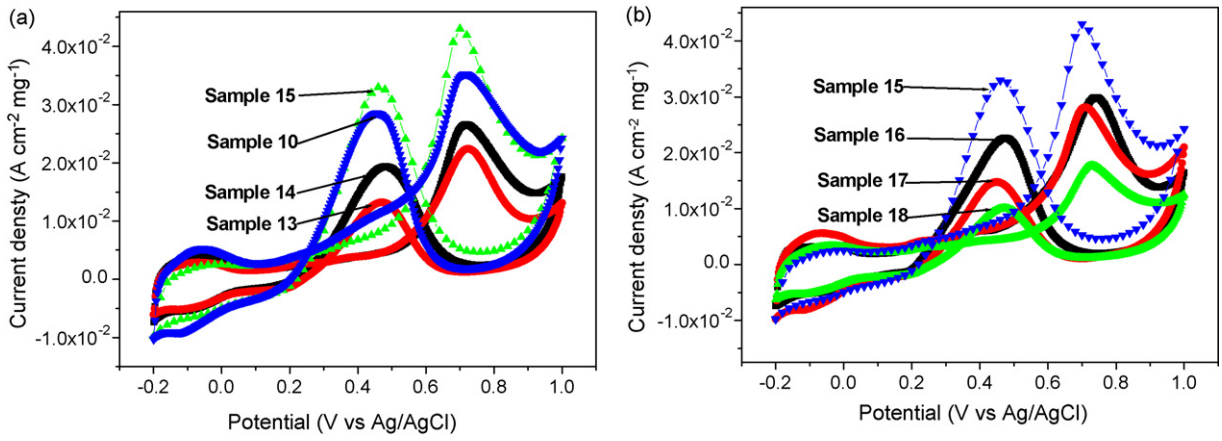

Fig. 7. Cyclic voltammograms of the Pt–Ru–PMo_{12}-MWNTs catalysts synthesized at a pH value of 7 in 0.5 M H_2SO_4 + 0.5 M CH_3OH electrolyte at the 125th cycle, collected at a scan rate of 200 mV s^{-1}: (a) effect of reaction time; (b) effect of microwave power.

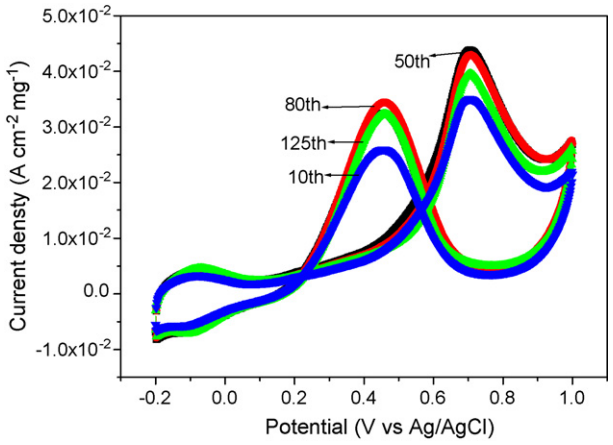

Fig. 8. Typical cyclic voltammogram curves (of sample 4) in 0.5 M H_2SO_4 + 0.5 M CH_3OH solution for different scan cycles, collected at a scan rate of 200 mV s^{-1}: (1) 10th cycle, (2) 50th cycle, (3) 80th cycle, and (4) 125th cycle.

the electrocatalytic properties of the Pt–Ru–PMo_{12}-MWNTs catalysts. The peak intensity of methanol oxidation increases first and then decreases with increasing microwave power. The electrochemical testing results show that the optimum pH value for the Pt–Ru–PMo_{12}-MWNTs catalysts is 7, in terms of its electrocatalytic activity and CO tolerance, which confirms that the pH value of the precursor solution dramatically affects the PtRu loading content and their crystallite size. So, Pt–Ru–PMo_{12}-MWNTs catalysts were synthesized at pH value of 7 under different reaction times and microwave powers. The cyclic voltammograms of the Pt–Ru–PMo_{12}-MWNTs catalysts synthesized at pH 7 in 0.5 M H_2SO_4 + 0.5 M CH_3OH solution at the 125th cycle are shown in Fig. 7(a) and (b). It is clearly observed that the intensity of the oxidation peaks increases with increasing reaction time. Sample 15, which was synthesized at a pH value of 7, shows the optimized electrocatalytic activity.

The long-term cycle stability of Pt–Ru–PMo_{12}-MWNTs is shown in Fig. 8, with sample 4 as an example. CV tests were conducted in 0.5 M H_2SO_4 + 0.5 M CH_3OH solution. Here the electrolyte solution is always refreshed with 0.5 M H_2SO_4 + 0.5 M CH_3OH after 10, 50, 80, and 125 cycles. From Fig. 8, it can be seen that the shape and peak potential of the curves show no evident changes, but the peak current first increases with the increasing number of cycles and then drops slightly as the cycle number continues to increase. One explanation is that there is an activation process for the Pt–Ru–PMo_{12}-MWNTs electrocatalysts in the beginning. The PMo_{12} monolayer covering the metal nanoparticles takes time to effectively work with Pt and Ru as a co-catalyst for methanol oxidation. However, part of the catalyst powder may drop off of the GC electrode after long cycling in the 0.5 M H_2SO_4 + 0.5 M CH_3OH solution, which induces current drop.

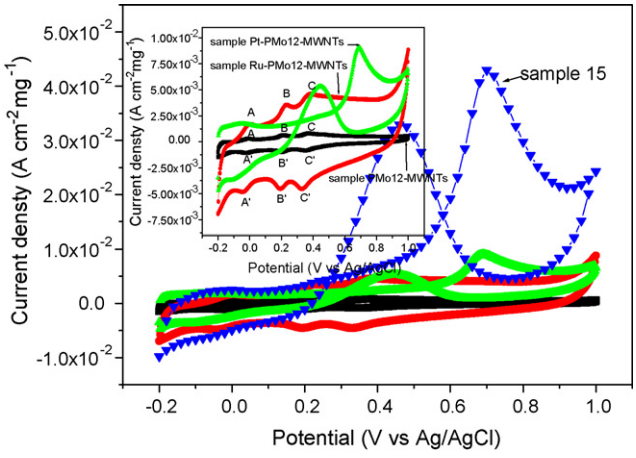

Fig. 9. Cyclic voltammogram curves of PMo_{12}-MWNTs, Ru–PMo_{12}-MWNTs, Pt–PMo_{12}-MWNTs, and Pt–Ru–PMo_{12}-MWNTs (sample 15), in 0.5 M H_2SO_4 + 0.5 M CH_3OH solution, collected at the 125th cycle at a scan rate of 200 mV s^{-1}. Inset shows enlarged cyclic voltammogram curves of the PMo_{12}-MWNT, the Ru–PMo_{12}-MWNT, and the Pt–PMo_{12}-MWNTs catalysts.

Fig. 9 compares cyclic voltammogram curves of PMo_{12}-MWNTs, Ru–PMo_{12}-MWNTs, Pt–PMo_{12}-MWNTs, and Pt–Ru–PMo_{12}-MWNTs. The cyclic voltammograms shown in Fig. 9 were collected at the 125th cycle using cells with 0.5 M H_2SO_4 + 0.5 M CH_3OH solution. There are no obvious methanol oxidation peaks for the PMo_{12}-MWNTs and Ru–PMo_{12}-MWNTs samples, but three pairs of peaks (A–A′, B–B′ and C–C′) for PMo_{12} can be clearly seen. For the Pt–PMo_{12}-MWNTs and Pt–Ru–PMo_{12}-MWNT samples, two methanol oxidation peaks can be clearly observed, which are located at about 0.7 V (forward scan) and 0.45 V (reverse scan), respectively. The voltammetric features are in good agreement with the literature [5,23]. The methanol oxidation current for the Pt–Ru–PMo_{12}-MWNTs is considerably higher than that of the Pt–PMo_{12}-MWNTs, indicating that the presence of Ru is important for the electrocatalytic activity towards methanol oxidation, due to the bifunctional mechanism.

In summary, the existence of PMo_{12} could effectively prevent the agglomeration of metal particles and MWNTs. The synthesized PtRu nanoparticles are dispersed very uniformly on the outer walls of the MWNTs with this synthesis method. Different preparation conditions of Pt–Ru–PMo_{12}-MWNTs catalysts were studied in this work. A sample prepared with a longer reaction time has a higher Pt loading content and shows higher electrochemical catalytic activity (Table 2 and Fig. 6(a)). High microwave power may accelerate the H_2PtCl_6 reduction reaction (Table 2), but it showed no evident effect on the electrochemical catalytic activity (Fig. 6(b)). The pH value is an important factor for catalyst preparation and can significantly affect the particle size and electrochemical catalytic activity of the catalysts. Sample 10 prepared at the pH value of 7 shows the best CO tolerance and promising electrocatalytic activity (Fig. 6(c)), and therefore, we think that the optimum pH value is 7 for the Pt–Ru–PMo_{12}-MWNTs preparation process using the microwave-assisted polyol method.

4. Conclusions

A novel catalyst with multiwalled carbon nanotubes (MWNT) as the support, Pt–Ru–PMo_{12}-MWNTs, was synthesized under different preparation conditions, by microwave heating of ethylene glycol solutions containing Pt and Ru salts, and PMo_{12}. The effects of the microwave reaction time, the microwave reaction power, and the pH value of the reaction solution on the performance of the Pt–Ru–PMo_{12}-MWNTs catalyst were investigated in our work. Polyoxometallate (PMo_{12}) can be chemically adsorbed on the surface of Pt, Ru nanoparticles, and on the outer walls of MWNTs. These effectively prevented the agglomeration of Pt and Ru nanoparticles due to the electrostatic repulsive interactions between the negatively charged PMo_{12} monolayers. Electrochemical measurements and EDS examination showed that the electrochemical activity and the loading content of Pt/Ru changed with the synthesis conditions. The electrochemical performance of Pt–Ru–PMo_{12}-MWNTs materials with different synthesis conditions was tested with CV in this work. It was found that the a Pt–Ru–PMo_{12}-MWNTs electrocatalyst with high Pt loading content, small crystallite size, and

good electrocatalytic activity could be synthesized with a long reaction time, intermediate microwave power, and a pH value of 7.

Acknowledgements

Financial support provided by the Wollongong University Research Council (URC) is gratefully acknowledged. This work was also financed by international cooperative research project grants for Ph.D. students of Sun Yat-Sen University. The authors also thank Dr. Silver Tania for editing the manuscript.

References

[1] F. Bensebaa, A.A. Farah, D. Wang, C. Bock, X.M. Du, J. Kung, Y.L. Page, J. Phys. Chem. B 109 (2005) 15339–15344.
[2] B. Yang, A. Manthiram, Electrochem. Commun. 6 (2004) 231–236.
[3] Z.L. Liu, L.M. Gan, L. Hong, W. Chen, J.Y. Lee, J. Power Sources 139 (2005) 73–78.
[4] X. Wang, I.M. Hsing, Electrochim. Acta 47 (2002) 2981–2987.
[5] X.Z. Xue, T.H. Lu, C.P. Liu, W.L. Xu, Y. Su, Y.Z. Lv, W. Xing, Electrochim. Acta 50 (2005) 3470–3478.
[6] R. Dillon, S. Srinivasan, A.S. Arico, V. Antonucci, J. Power Sources 127 (2004) 112–126.
[7] K.W. Weng, S. Han, Y.L. Chen, Y.C. Chen, D.Y. Wang, Surf. Coat. Technol. 201 (2007) 6557–6560.
[8] H.S. Liu, C.J. Song, L. Zhang, J.J. Zhang, H.J. Wang, D.P. Wilkinson, J. Power Sources 155 (2006) 95–110.
[9] A.S. Arico, S. Srinivasan, V. Antonucci, Fuel Cells 2 (2001) 133–161.
[10] C. Lamy, J.M. Leger, S. Srinivasan, J.O.M. Bockris, B.E. Conway, R.E. White (Eds.), Modern Aspects of Electrochemistry, vol. 34, Kluwer Academic/plenum publisher, New York, 2001, pp. 53–118.
[11] E. Ticianelli, J.G. Berry, M.T. Paffet, S. Gottesfeld, J. Electroanal. Chem. 81 (1977) 229–238.
[12] M. Watanabe, S. Motoo, J. Electroanal. Chem. 60 (1975) 267–273.
[13] T.W. Ebbesen, H.J. Lezec, H. Hiura, J.W. Bennett, H.F. Ghaemi, T. Thio, Nature 382 (1996) 54–56.
[14] R.H. Baughman, A.A. Zakhidov, W.A. Heer, Science 297 (2002) 787–792.
[15] K.M. Lee, L.C. Li, L.M. Dai, J. Am. Chem. Soc. 127 (2005) 4122–4123.
[16] A. Kuhn, F.C. Anson, Langmuir 12 (1996) 5481–5488.
[17] M. Ge, B. Zhong, W.G. Klemperer, A.A. Gewirth, J. Am. Chem. Soc. 118 (1996) 5812–5813.
[18] M. Gotz, H. Wendt, Electrochim. Acta 43 (1998) 3637–3644.
[19] C. Lamy, J.M. LØger, in: O. Savadogo, P.R. Roberge (Eds.), Proceedings of the Second International Symposium on New Materials for Fuel Cells and Modern Battery Systems, Montreal, Canada, 1997, pp. 477–487.
[20] Z.P. Guo, D.M. Han, D. Wexler, R. Zeng, H.K. Liu, Electrochim. Acta, in press.
[21] Z.P. Guo, Z.W. Zhao, H.K. Liu, S.X. Dou, Carbon 43 (2005) 1392–1399.
[22] P.J. Kulesza, K. Karnicka, K. Miecznikowski, M. Chojak, A. Kolary, P.J. Barczuk, G. Tsirlina, W. Czerwinski, Electrochim. Acta 50 (2005) 5155–5162.
[23] Y.Y. Mu, H.P. Liang, J.S. Hu, L. Jiang, L.J. Wan, J. Phys. Chem. B 109 (2005) 22212–22216.
[24] D.L. Wang, L. Zhuang, J.T. Lu, J. Phys. Chem. C 111 (2007) 16416–16422.
[25] J.S. Guo, G.Q. Sun, S.G. Sun, S.Y. Yan, W.Q. Yang, J. Qi, Y.S. Yan, Q. Xin, J. Power Sources 168 (2007) 299–306.
[26] Z.B. Wang, G.P. Yin, P.F. Shi, B.Q. Yang, P.X. Feng, J. Power Sources 166 (2007) 317–323.
[27] Z.L. Liu, X.Y. Ling, X.D. Su, J.Y. Lee, J. Phys. Chem. B 108 (2004) 8234–8240.